Unimolecular dissociation of the propargyl radical intermediate of the $CH+C_2H_2$ and $C+C_2H_3$ reactions

Laura R. McCunn,[a] Benjamin L. FitzPatrick, Maria J. Krisch,[b] and Laurie J. Butler[c]
The James Franck Institute and Department of Chemistry, University of Chicago, Chicago, Illinois 60637

Chi-Wei Liang and Jim J. Lin
Institute of Atomic and Molecular Sciences, Academia Sinica, Taipei, Taiwan 106 Republic of China

(Received 14 April 2006; accepted 18 August 2006; published online 2 October 2006)

This paper examines the unimolecular dissociation of propargyl ($HCCCH_2$) radicals over a range of internal energies to probe the $CH+HCCH$ and $C+C_2H_3$ bimolecular reactions from the radical intermediate to products. The propargyl radical was produced by 157 nm photolysis of propargyl chloride in crossed laser-molecular beam scattering experiments. The H-loss and H_2 elimination channels of the nascent propargyl radicals were observed. Detection of stable propargyl radicals gave an experimental determination of 71.5 (+5/−10) kcal/mol as the lowest barrier to dissociation of the radical. This barrier is significantly lower than predictions for the lowest barrier to the radical's dissociation and also lower than calculated overall reaction enthalpies. Products from both H_2+HCCC and $H+C_3H_2$ channels were detected at energies lower than what has been theoretically predicted. An HCl elimination channel and a minor C–H fission channel were also observed in the photolysis of propargyl chloride. © *2006 American Institute of Physics*.
[DOI: 10.1063/1.2353821]

INTRODUCTION

The propargyl ($HCCCH_2$) radical occupies the minimum of the C_3H_3 potential energy surface and is involved in reactions relevant to interstellar chemistry and combustion.[1,2] It has been predicted to be an intermediate occurring in both the $C+C_2H_3$ and $CH+C_2H_2$ reactions, which can ultimately produce various isomers of C_3H_2 and C_3H. Both C_3H_2 and C_3H have been detected in the interstellar medium.[3–6] The mechanisms of formation for these radicals are unclear, but the propargyl radical has been suggested as a forerunner to these species.[7] In combustion processes, the combination of two propargyl radicals makes the first aromatic ring leading to the formation of polycyclic aromatic hydrocarbons and soot.[8] Besides the applications to combustion and astrochemistry, the unimolecular dissociation of the propargyl radical is interesting in its own right because the dynamics involve several dissociation and isomerization channels, as well as an excited electronic state.

In one of the earliest experiments on the propargyl radical, Ramsay and Thistlethwaite[9] recorded the UV absorption spectrum. They recorded a set of diffuse bands in the range of 290–345 nm following the flash photolysis of propargyl chloride, propargyl bromide, propyne, allene, and other molecules. The bands were assigned to propargyl and set an upper bound for the radical's lowest bond dissociation energy at $D_0 \leqslant 86.04$ kcal/mol. In another determination of bond dissociation energy, Robinson *et al.*[10] measured the gas phase acidity of the propargyl radical and the electron affinity of H_2CCC. From these two quantities, they deduced that the bond dissociation energy for H_2CCC-H to form $H+H_2CCC$, the highest-energy C_3H_2 product isomer, is 100 ± 5 kcal/mol.

The ionization potential of 8.68 eV for the propargyl radical is well established.[11–13] High-resolution photoionization studies have identified it as an important intermediate in several combustion flames.[14] Experiments by various groups have recorded the photoionization cross section,[15] and the infrared[16] and ultraviolet[9,17] absorption spectra. The excited-state decay of propargyl has been characterized by femtosecond time-resolved photoionization.[18] An exponential decay time constant of 50 ± 10 fs was measured for the radical in the $3\,^2B_1$ state. This state is predicted to lie 5.12 eV above the ground state, inaccessible for the radicals produced in the experiments presented here. Electronic spectra of the propargyl radical isolated in a neon matrix assigned bands to the $A\,^2A''$ and $B\,^2A'$ states at 3.52 and 3.61 eV, respectively.[19]

The dissociation of the propargyl radical, including photochemical and unimolecular ground-state surface processes, has been studied extensively as a solitary reaction and also as a part of other chemical processes. Deyerl *et al.*[20] photodissociated the propargyl radical at wavelengths from 265 to 240 nm and detected H products. They assigned the products to the $H+c\text{-}C_3H_2$ channel with rates in agreement with Rice-Ramsperger-Kassel-Marcus (RRKM) predictions. A later paper[21] found that these results are also consistent with fast isomerization of propargyl radicals prior to dissociation to $H+HCCCH$. Photodissociation of monodeuterated propargyl (H_2CCCD) showed nearly complete isotopic scrambling, in accordance with formation of $c\text{-}C_3H_2$ via a [1,2] H shift and cyclization followed by H loss.

[a]Present address: Department of Chemistry, Yale University, P.O. Box 208107, New Haven, CT 06520.
[b]Present address: Department of Chemistry, University of California, Irvine, CA 92697.
[c]Electronic mail: l-butler@uchicago.edu

 © 2006 American Institute of Physics

Downloaded 25 Oct 2006 to 128.135.186.84. Redistribution subject to AIP license or copyright, see http://jcp.aip.org/jcp/copyright.jsp

Vereecken *et al.*[22] used the B3LYP-DFT/6-31G** method to investigate features of the $CH(X\,^2\Pi)+C_2H_2$ reaction, of which the propargyl intermediate is the energetic minimum. Energies were verified by CASPT2 calculations. Mapping of the H_2 elimination and H loss channels of the propargyl radical showed that singlet cyclopropenylidene +H products are energetically favored. All three H-loss channels were found to be barrierless. Vibrational modes for all stationary points and transition states were calculated. In a subsequent paper,[23] the density functional theory (DFT) and CASPT2 results were used for temperature- and pressure-dependent RRKM analyses. Calculated product distributions predicted that H+HCCCH would be the dominant products (>80%), regardless of whether the initial reaction proceeds through chain addition, cycloaddition, or insertion. Collisional stabilization of the propargyl radical becomes prevalent at high pressures.

Another RRKM study of $CH(X\,^2\Pi)+C_2H_2$ by Guadagnini *et al.* is applicable in the low-pressure regime.[24] Using geometries determined at the complete active space self-consistent field (CASSCF) level, this paper used internally contracted configuration interaction (CI) calculations to determine energetic barriers to the HCCCH+H and H_2CCC+H product channels in propargyl dissociation, as well as several other minima and transition states. At this level of theory, the electronic structure calculations predict that the asymptotic energy of the H_2CCC+H product channel is quite similar to that of HCCCH+H and that the latter has a substantial exit barrier. Because of this difference, the RRKM calculations showed that the product branching yields essentially 100% H_2CCC. H_2 elimination and $H+c\text{-}C_3H_2$ product channels were excluded from the RRKM analysis in this paper.

The most comprehensive theoretical work thus far on the potential energy surface of the $C+C_2H_3$ and $CH+C_2H_2$ reactions is in two recent papers by Mebel and co-workers.[21,25] Nguyen *et al.*[25] examined the $C(^3P)+C_2H_3(^2A')$ reaction using B3LYP/6-311G(*d*,*p*) and RCCSD(T)/6-311+G(3*df*,2*p*) methods. The reaction occurs on the same surface as the $CH+C_2H_2$ reaction with propargyl as the minimum-energy radical intermediate. Nguyen *et al.* found the three H-loss channels of propargyl to be barrierless, as Vereecken *et al.*[22] had found previously. Thermochemistry for C_3H_n (n=1–4) species was investigated. In addition, energetics for the excited states of various C_3H_3 radical isomers were calculated by CASSCF and multireference configuration interaction (MRCI) methods. The propargyl radical was found to have an adiabatic excitation energy of 57.1 kcal/mol. In a subsequent paper, Nguyen *et al.*[21] used RRKM calculations based on the $C(^3P)+C_2H_3(^2A')$ and $CH(^2\Pi)+C_2H_2(^1\Sigma_g^+)$ energetics to predict branching for each of the two reactions. In both cases, the major products were predicted to be $HCCCH(^3B)$+H (>80%), similar to the branching ratio for $CH(^2\Pi)+C_2H_2$ predicted by Vereecken and Peeters.[23] Nguyen *et al.* also simulated the 193 and 242 nm photolysis of propargyl radical. Again, assuming that the propargyl radicals undergo internal conversion to the ground electronic state, $HCCCH(^3B)$+H were predicted to be the major products, 86.5% for photolysis at 193 nm and 90.2% at 242 nm. Deyerl *et al.*[20] had previously found $c\text{-}C_3H_2$+H to be the major products based on isotopic scrambling in the 242 nm photolysis of deuterated propargyl, but Nguyen *et al.*[21] demonstrated that the relatively fast isomerization of propargyl radicals could easily account for isotopic scrambling prior to the $HCCCH_2 \rightarrow HCCCH+H$ reaction.

Allene (H_2CCCH_2) and propyne ($HCCCH_3$) have been studied as photolytic sources of the propargyl radical. Crossed laser-molecular beam experiments on allene photodissociation at 193 nm revealed two primary processes: H loss (89%) and H_2 elimination (11%).[26] The C_3H_3 and C_3H_2 products from primary photodissociation each absorbed an additional 193 nm photon and underwent secondary photodissociation, including H loss, H_2 elimination, and C–C bond fission. The different product isomers could not be resolved and identified in these experiments. *Ab initio* calculations by Mebel *et al.*[27] mapped the primary and secondary photodissociation channels of allene and propyne. Recently, H (Rydberg) atom photofragment translational spectroscopy confirmed that the photolysis of each of the two molecules in the near-UV produces propargyl radicals.[28] The mechanism of allene and propyne photolysis is best explained by absorption followed by internal conversion, isomerization, and dissociation on the ground-state potential energy surface. A second study[29] with photolysis at 193.3 and 121.6 nm confirmed the same mechanism. At 121.6 nm, however, a fraction of propyne molecules can dissociate from an excited state to make the 1-propynyl radical instead of propargyl.

Unimolecular dissociation of propargyl can lead to various isomers of C_3H_2, so accurate relative energies of the isomers are important to understand the propargyl radical's dissociation dynamics. Various theoretical works have focused on calculating the energetics of C_3H_2 isomers. Multiconfigurational second-order perturbation calculations on C_3H_2 found that the singlet cyclopropenylidene isomer is lowest in energy, followed by triplet propargylene (^{3}HCCCH), singlet propadienylidene (^1H_2CCC), singlet propargylene (^{1}HCCCH), and triplet propadienylidene (^3H_2CCC).[30] This is the same order of stability found in other *ab initio* studies.[31–34]

In this paper, we seek to shed light on the $C+C_2H_3$ and $CH+C_2H_2$ reactions by directly probing the propargyl radical intermediate. The experiments are designed to produce propargyl radicals dispersed by internal energy and to monitor dissociation of the radicals as a function of internal energy. It has been shown that the isomerization of C_3H_3 radical intermediates to propargyl is relatively fast in the $C+C_2H_3$ and $CH+C_2H_2$ reactions,[21] so our experiment serves to probe the fate of propargyl radical intermediates in these reactions in the absence of secondary bimolecular collisions. This provides a more stringent test of theory in the determination of reaction energetics and dynamics. Propargyl chloride is the photolytic precursor for the propargyl radical in these experiments. The photolysis wavelength of 157 nm was deliberately chosen to produce nascent propargyl radicals with a range of internal energies that spanned the various barriers to dissociation. Previous experiments[35] using 193 nm, rather than 157 nm, to photodissociate propargyl

Downloaded 25 Oct 2006 to 128.135.186.84. Redistribution subject to AIP license or copyright, see http://jcp.aip.org/jcp/copyright.jsp

chloride showed that the nascent propargyl radicals do not have sufficient energy to access unimolecular dissociation channels following the 193 nm photolysis. The following are the available photolysis channels for propargyl chloride at 157 nm, with the secondary dissociation processes indented. The energetics given below are from the referenced computational studies.

$$HC{\equiv}CCH_2Cl \rightarrow HCCCH_2 + Cl,$$
$$\Delta H_{0\ K} = 66.9 \text{ kcal/mol} \quad \text{(Refs. 36 and 37)} \tag{1}$$

$$HCCCH_2 \rightarrow HCCC + H_2,$$
$$\Delta H_{0\ K} = 84.0 \text{ kcal/mol} \quad \text{(Ref. 25)}, \tag{2}$$

$$HCCCH_2 \rightarrow HCCCH + H,$$
$$\Delta H_{0\ K} = 94.9 \text{ kcal/mol} \quad \text{(Ref. 25)}, \tag{3}$$

$$HCCCH_2 \rightarrow H_2C{=}C{=}C + H,$$
$$\Delta H_{0\ K} = 95.9 \text{ kcal/mol} \quad \text{(Ref. 25)}, \tag{4}$$

$$HCCCH_2 \rightarrow c - C_3H_2 + H,$$
$$\Delta H_{0\ K} = 82.4 \text{ kcal/mol} \quad \text{(Ref. 25)}, \tag{5}$$

$$HCCCH_2 \rightarrow C_2H_2 + CH,$$
$$\Delta H_{0\ K} = 109.0 \text{ kcal/mol} \quad \text{(Ref. 22)}, \tag{6}$$

$$HC{\equiv}CCH_2Cl \rightarrow HCCCH + HCl,$$
$$\Delta H_{0\ K} = 59.5 \text{ kcal/mol} \quad \text{(Ref. 38)}, \tag{7}$$

$$HC{\equiv}CCH_2Cl \rightarrow HCCCHCl + H,$$
$$\Delta H_{0\ K} = 83 \text{ kcal/mol} \quad \text{(Ref. 39)}, \tag{8}$$

$$HC{\equiv}CCH_2Cl \rightarrow CCCH_2Cl + H,$$
$$\Delta H_{0\ K} = 127 \text{ kcal/mol} \quad \text{(Ref. 39)}. \tag{9}$$

In the experiments presented here, C_3H_2 isomers are likely products from the unimolecular dissociation of propargyl and also from the HCl elimination channel of the propargyl chloride precursor. Tunable synchrotron photoionization is useful in resolving isomers with dissimilar ionization energies. Such an approach has been used in an attempt to identify C_3H_2 isomers sampled from a rich cyclopentene flame.[34] Unfortunately, the ionization energies of propargylene (HCCCH) (8.96 eV) (Ref. 34) and cyclopropenylidene (c-C_3H_2) (9.1 eV) (Ref. 40) are sufficiently close that the two radicals cannot be resolved. The case is simpler for propadienylidene (H_2CCC), which can be distinguished from the other two isomers by its higher ionization potential of 10.43 eV.[40] Differences in the shapes of the time-of-flight distributions for C_3H_2 produced by propargyl dissociation and by HCl elimination of propargyl chloride make it possible to identify C_3H_2 products from these two sources.

EXPERIMENTAL METHOD

The velocities of the primary photofragments of propargyl chloride photolysis and the products of the unimolecular dissociation of the C_3H_3 radicals were measured with the rotating-source crossed laser-molecular beam apparatus on the 21A1 U9/Chemical Dynamics Beamline at the National Synchrotron Radiation Research Center (NSRRC) in Hsinchu, Taiwan. A 7% propargyl chloride-Ne molecular beam was created by bubbling neon (1000 Torr total backing pressure) through propargyl chloride (98% purity, Sigma-Aldrich) cooled to 0.0 °C and expanding the mixture through an Even-Lavie pulsed valve having a 0.4 mm orifice operating at 100 Hz. The nozzle was heated to 120 °C to reduce cluster formation. The molecular beam of the parent molecule was characterized by directing the beam through a chopper wheel along the detector axis. The measured number-density speed distribution of the propargyl chloride molecular beam for the data presented here was typically peaked at 7.7×10^4 cm/s with a full width at half maximum of 19%.

Photodissociation was accomplished by a Lambda Physik LPF 220 F_2 laser operating at 157.6 nm. The laser ran at 100 Hz with a pulse energy between 1 and 3 mJ/pulse, which is below the saturation level of propargyl chloride, to avoid multiphoton processes. The pulse energy varied over the course of the experiments, but a specific value was recorded for each individual spectrum. The laser beam was focused to an area of 1.5 mm wide by 8.5 mm high, intersecting the ~3 mm high molecular beam at a 90° angle in the interaction region. Photofragments recoiling in the direction of the detector traveled 10.05 cm to the ionizing region, where tunable vacuum ultraviolet (VUV) synchrotron radiation ionized a portion of the fragments. Photoionization energies were selected by tuning the gap of a U9 undulator, which generated the radiation. For example, Cl^+ data were collected at $m/e=35$ using a 14.8 eV photoionization energy, requiring a 34 mm undulator gap. Unwanted higher harmonics of VUV radiation were removed by a rare gas filter. The VUV beam was defined by a circular aperture of 7 mm diameter for a full width at half maximum of 0.27 eV, or 3%.

Ionized photofragments were mass selected by an Extrel 2.1 MHz quadrupole mass spectrometer and then counted by a Daly detector. A multichannel scaler was used to record the total time of flight (TOF) of the photofragments from the interaction region to the detector. Recoil translational energy distributions were found by forward convolution fitting of the TOF spectra. The forward convolution fitting of the data accounted for the ion flight time, derived from the apparatus' ion flight constant of 5.45 μs amu$^{-1/2}$. The experimental data and fits shown in this paper have already subtracted the 1.225 μs delay between the trigger of the multichannel scaler and the arrival of the laser pulse at the interaction region.

Supplemental data were taken on the crossed laser-molecular beam apparatus at the Institute for Atomic and Molecular Sciences (IAMS), Academia Sinica, Taiwan. This apparatus uses 70 eV electron bombardment for photofragment ionization, but is otherwise similar to the NSRRC ap-

Downloaded 25 Oct 2006 to 128.135.186.84. Redistribution subject to AIP license or copyright, see http://jcp.aip.org/jcp/copyright.jsp

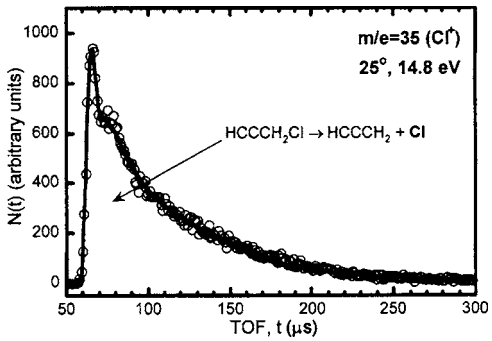

FIG. 1. Time of flight (TOF) spectrum of $m/e=35$ (Cl^+) taken at a source angle of 25° and ionization energy of 14.8 eV for 100 000 laser shots. The open circles represent experimental data points while the solid line is the overall forward convolution fit to the data with the thin solid line $P(E_T)$ shown in Fig. 2.

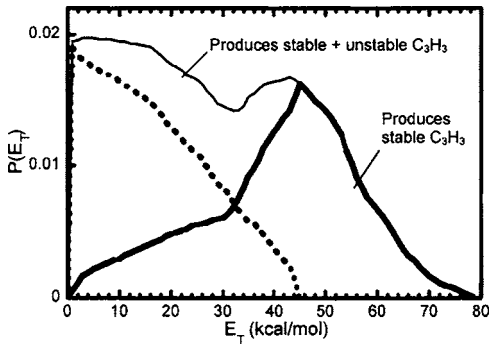

FIG. 2. Recoil kinetic energy distribution, $P(E_T)$, in C–Cl bond fission of propargyl chloride. The thin solid line shows the total $P(E_T)$, derived in the forward convolution fitting of the data in Fig. 1. This $P(E_T)$ is divided into two subdistributions used in fitting of subsequent spectra. The bold solid line corresponds to high E_T, low E_{int}, C_3H_3 radicals that are stable to unimolecular dissociation; this is derived in the forward convolution fitting of the data shown in Fig. 5. The dotted line corresponds to low E_T, high E_{int}, C_3H_3 radicals that do dissociate, deduced from the difference between the thin solid and bold solid lines.

paratus. Only the major differences between the apparatus at IAMS and the one at NSRRC are described here. The flight path length from the laser interaction region to the detector was 24.2 cm, and photofragments were ionized by a 70 eV electron bombardment ionizer instead of vuv radiation. An ion flight constant of 4.6 μs $amu^{-1/2}$ was used for fitting data from this instrument. A 2.5 μs delay between the triggering of the multichannel scaler and the firing of the 157 nm excimer laser has been subtracted from the IAMS data. All figures in this paper present data from NSRRC, unless noted as IAMS laboratory data.

RESULTS AND ANALYSIS

The data showed that C–Cl bond fission was the major photodissociation channel of propargyl chloride at 157 nm. The UV absorption spectrum of propargyl chloride has been recorded by Fahr *et al.*[17] down to 160 nm, where it has a cross section of 1×10^{-17} cm^2. In the experiments presented here, strong absorption was observed at 157 nm. C–Cl fission was evidenced by a Cl^+ TOF spectrum at $m/e=35$ with a source angle of 25° shown in Fig. 1. The total recoil kinetic energy distribution $P(E_T)$ for C–Cl fission was determined by forward convolution fitting of the data. The total $P(E_T)$ is bimodal as shown by the thin solid line in Fig. 2, with the broad low-energy component peaking below 5 kcal/mol. The bimodal nature could be attributed to the low kinetic energy C–Cl bond fission channel producing propargyl radicals in an excited electronic state. Subsequent analysis of $m/e=39$ ($C_3H_3^+$) data revealed that a portion of the propargyl radicals formed in C–Cl fission was stable to dissociation. The total C–Cl fission $P(E_T)$ was divided to reflect this. The bold solid line in Fig. 2 corresponds to C–Cl fission events producing propargyl radicals that were stable to dissociation as reasoned below in the fitting of Fig. 5. The dotted line, obtained from the difference of the thin solid line [$P(E_T)$ for all C–Cl bond fission events] and the bold solid line [$P(E_T)$ for C_3H_3 not lost to unimolecular dissociation], corresponds to C–Cl bond fission events that produced propargyl radicals that were not subsequently detected as stable. Thus, these propargyl radicals had sufficient energy to dissociate to H_2 +HCCC or H+C_3H_2.

A TOF spectrum for $m/e=36$ ($H^{35}Cl^+$,C_3^+) at a 25° source angle indicated the presence of a HCl elimination channel, shown by the dashed line in Fig. 3. The HCl product distribution was fitted by the $P(E_T)$ in Fig. 4. Also present in the $m/e=36$ TOF is a small contribution from C_3^+ arising from dissociative ionization of stable propargyl radicals, shown by the thin solid line in Fig. 3. To estimate the branching ratio between C–Cl bond fission and HCl elimination, we integrated the signal in the background-subtracted Cl^+ and HCl^+ TOF spectra. The spectra were collected under identical molecular beam conditions and photolysis laser power with the same ionization energy (14.8 eV) and photoflux from the synchrotron. The $m/e=35$ (Cl^+) TOF spectrum shown in Fig. 1 was integrated in the range of 57–300 μs. The HCl product distribution in the $m/e=36$ (HCl^+,C_3^+) TOF spectrum shown in Fig. 3 was integrated from 65 to 300 μs, counting only the HCl signal. The ratio of the integrated signals was corrected by the photoionization cross sections, $\sigma_{ion}=46$ Mb for HCl and $\sigma_{ion}=28$ Mb for Cl at 14.8 eV.[41,42] Accounting for the appropriate Jacobian factors gave a [Cl]/[HCl] branching ratio of 6.8, or ~87% branching to

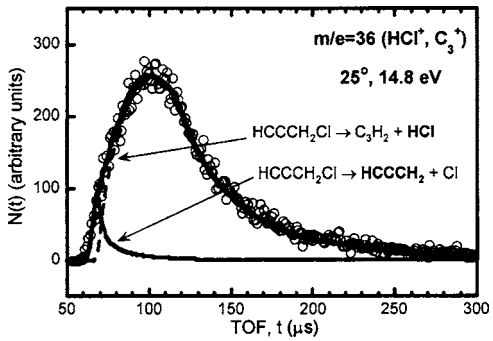

FIG. 3. TOF spectrum of $m/e=36$ (HCl^+,C_3^+) taken at a 25° source angle, obtained from 100 000 laser shots and an ionization energy of 14.8 eV. Open circles are experimental data and the bold line is the total fit. The dashed line shows the HCl product distribution and the thin solid line shows stable C_3H_3 radicals that undergo dissociative ionization to C_3^+. The latter is calculated from the stable propargyl radical $P(E_T)$ in Fig. 2, derived from $m/e=39$ signal in Fig. 5.

Downloaded 25 Oct 2006 to 128.135.186.84. Redistribution subject to AIP license or copyright, see http://jcp.aip.org/jcp/copyright.jsp

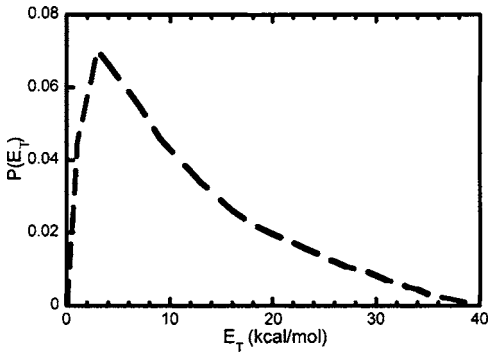

FIG. 4. Recoil translational energy distribution, $P(E_T)$, in HCl elimination of propargyl chloride. This $P(E_T)$ is determined from forward convolution fitting of the data in Fig. 3.

C–Cl bond fission. We assume that both products have the same angular anisotropy (the $1+\beta/4$ correction factor for the experiment done with unpolarized laser light is small even if the products have different anisotropies).

Stable propargyl radicals were observed in $m/e=39$ TOF spectra at several ionization energies (Fig. 5). The data show that the photoionization cross section of C_3H_3 is dependent on the radical's internal energy. At a photoionization energy of 10.3 eV [Fig. 5(a)], the slower C_3H_3 products are ionized preferentially compared to the faster C_3H_3. This may be a sign that some of the propargyl radicals are produced in an excited electronic state with a lower ionization energy. Upon first inspection, it seems that many of the faster C_3H_3 radicals in the $m/e=39$ TOF distribution are 1-propynyl (CH_3CC) radicals, which have a higher ionization energy of 10.57 eV (corresponding to the triplet state of the ion).[43] However, although some propargyl radicals with high internal energy can isomerize, the fraction in the 1-propynyl form would be quite small.[25] The difference in the $m/e=39$ TOF spectra at 10.3 and 11.9 eV may be explained more accurately by the presence of excited-state propargyl radicals. Higher ionization energies are sufficient to ionize the faster C_3H_3 products. A satisfactory fit to data taken at 11.9 eV is shown in Fig. 5(b). TOF distributions nearly identical to Fig. 5(b) were observed at photoionization energies up to 14 eV. This suggests that by 11.9 eV, the photoionization energy of the radicals is roughly independent of internal energy. Thus, the $P(E_T)$ fitting the spectrum in Fig. 5(b) is taken as a faithful representation of stable propargyl radicals. Data taken with 70 eV electron bombardment ionization at the IAMS facility [Fig. 5(c)] are very well fitted by the $P(E_T)$ for the 11.9 eV data. It does, however, reveal additional signal in the 120–150 μs TOF range. This signal adds a small but distinct peak in the spectrum. Possible sources of this peak include clusters in the molecular beam or some chemical contaminant in the propargyl chloride sample. We did attempt to fit the full TOF distribution in Fig. 5(c) as stable C_3H_3 radicals, but that resulted in a distribution for the unstable radicals that did not fit the $m/e=37$ and $m/e=38$ products of dissociation.

The data in Fig. 5 were fitted with the high kinetic energy portion of the C–Cl bond fission $P(E_T)$, shown by the bold solid line in Fig. 2. Only the high kinetic energy part of

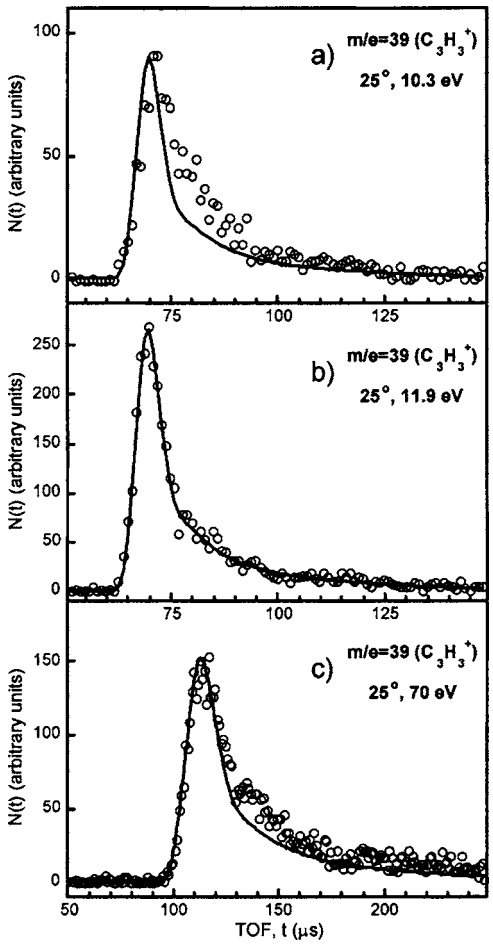

FIG. 5. TOF spectra of $m/e=39$ ($C_3H_3^+$) taken at a 25° source angle for 50 000 laser shots with (a) 10.3 eV photoionization, (b) 11.9 eV photoionization, and (c) 70 eV electron bombardment ionization. The TOF distribution in (c) exhibits longer flight times because it was taken on a separate apparatus with a longer neutral flight path. Open circles are experimental data points and the solid line is the forward convolution fit to the data obtained from the component of the $P(E_T)$ in Fig. 2 shown in bold solid line. The recoil kinetic energy distribution for the data is described by the bold solid line in Fig. 2, which shows that propargyl radicals begin to dissociate when $E_T=45$ kcal/mol.

the total C–Cl bond fission $P(E_T)$ was used, as the Cl atoms with low recoil kinetic energy correspond to C_3H_3 radicals with internal energies sufficient to overcome the barrier to dissociation, meaning that they would not be detected at $m/e=39$. The unstable radicals were formed from C–Cl bond fission imparting lower recoil kinetic energies to the two fragments as shown by the portion of the E_T distribution marked by the dotted line in Fig. 2. The E_T marking the onset of dissociation of the unstable propargyl radicals [45(+10/−5) kcal/mol] provides an experimental determination of the lowest-energy barrier to dissociation of these radicals, as described in the Discussion. Note that fitting the extra signal in Fig. 5(c) would not substantially change this barrier value of E_T.

Determination of the fit to the C_3H_3 TOF data is important because the point where the C_3H_3 $P(E_T)$ diverges from the total C–Cl bond fission $P(E_T)$ gives the value of E_T that is used to calculate the energy barrier to dissociation of C_3H_3. To test the reliability of the onset value of E_T

Downloaded 25 Oct 2006 to 128.135.186.84. Redistribution subject to AIP license or copyright, see http://jcp.aip.org/jcp/copyright.jsp

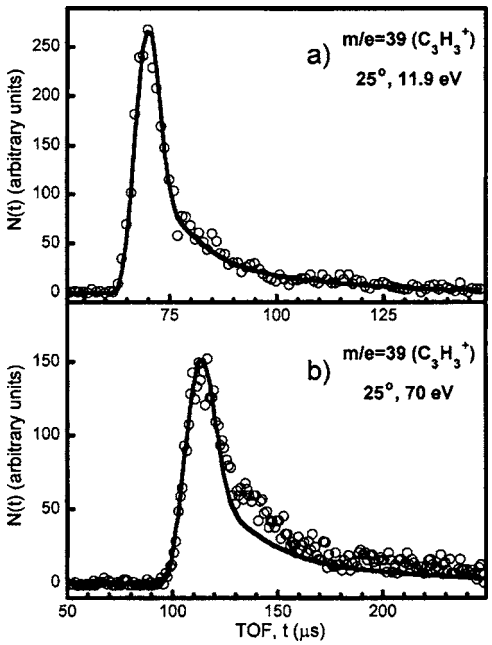

FIG. 6. TOF spectra of $m/e=39$ ($C_3H_3^+$) taken at a 25° source angle for 50 000 laser shots with (a) 11.9 eV photoionization and (b) 70 eV electron bombardment ionization. The data are identical to those in Fig. 5, but are fitted with the condition that dissociation of propargyl radicals onsets at $E_T=40$ kcal/mol.

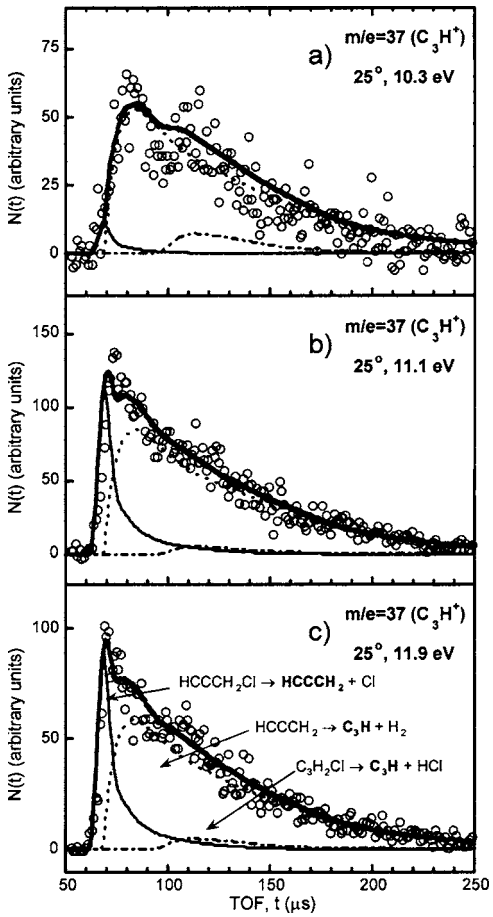

FIG. 7. TOF spectra of $m/e=37$ (C_3H^+) obtained at a 25° source angle with (a) 10.3 eV photoionization and 300 000 laser shots, (b) 11.1 eV photoionization and 300 000 laser shots, and (c) 11.9 eV photoionization and 50 000 laser shots. In each spectrum, the open circles are experimental data points and the bold solid line is the total fit to the data. The dotted line shows C_3H produced by H_2 elimination from unstable C_3H_3 radicals. The thin solid line shows signal from dissociative ionization of stable C_3H_3 radicals. The dot-dashed line shows C_3H formed by dissociation of C_3H_2Cl, which is initially formed by H loss from propargyl chloride.

=45 kcal/mol found above, we refitted the $m/e=39$ data to see how much we could change this value of E_T that marks the onset of radical dissociation. Figure 6 shows such a fit to two $m/e=39$ TOF spectra when dissociation onsets at $E_T=40$ kcal/mol. Attempts to use values of E_T lower than 40 kcal/mol yielded unacceptable fits. Note that using $E_T=40$ kcal/mol in a calculation of the dissociation barrier will give a result 5 kcal/mol higher than if $E_T=45$ kcal/mol is used. To be thorough, we also tried fitting the data with higher values of E_T marking the barrier. We could make satisfactory fits with the barrier at E_T up to 50 kcal/mol, but this would effectively lower the experimentally determined barrier. A lower barrier seems unlikely, as explained in the Discussion.

The elimination of H_2 from nascent propargyl radicals [reaction (2)] was observed in the $m/e=37$ (C_3H^+) TOF spectra. Figure 7 shows fits to the TOF data taken at three different ionization energies. In order to be sure that the signal in this TOF spectrum is truly due to C_3H, the possibility of dissociative ionization of C_3H_2 must be ruled out. The appearance energy of C_3H^+ from C_3H_2 could not be found in the literature; however, a mass spectrometric study with 10.5 eV photoionization of three C_3H_2 isomers revealed no appreciable signal at $m/e=37$.[40] Therefore, we have confidence in assigning the $m/e=37$ signal to reaction (2), and not reaction (3) and (4), or (5), based on signal observed in our experiments at a photoionization energy of 10.3 eV [Fig. 7(a)]. This is well above the ionization potential of 9.06 eV predicted[44] for the most stable isomer, cyclic C_3H. We cannot distinguish between C_3H isomers here, but the linear isomer is only 1 kcal/mol higher in energy than the cyclic isomer.[44] During H_2 elimination from unstable propargyl radicals, conservation of momentum dictates that the light H_2 molecule leaves with high velocity, while little velocity is imparted to the heavy C_3H fragment. Therefore, C_3H has a velocity virtually unchanged from the original propargyl radical. It is reasonable to predict the TOF distribution of C_3H products using the $P(E_T)$ corresponding to unstable C_3H_3 fragments, shown by the dotted line in Fig. 2. In all three TOF spectra in Fig. 7, the dotted line shows the distribution of C_3H^+ that originates from C_3H produced in reaction (2), assuming that this channel is accessed from propargyl radicals across the internal energy distribution determined from the dotted line $P(E_T)$ in Fig. 2. (Note that this result is inconsistent with a high exit barrier calculated for this channel.[25]) It is evident that dissociative ionization of stable C_3H_3 radicals contributes to the $m/e=37$ spectra at 11.1 and 11.9 eV in Figs. 7(b) and 7(c), respectively. The thin solid line shows the appearance of C_3H^+ from dissociative ionization of stable C_3H_3 radicals. The relative contribution of stable C_3H_3 increases with photoionization energy. Finally, C_3H_2Cl fragments, formed from initial H loss from propargyl chloride [reaction (8) or (9)], can dissociate and make C_3H. The dot-dashed line shows a possible fit for this

Downloaded 25 Oct 2006 to 128.135.186.84. Redistribution subject to AIP license or copyright, see http://jcp.aip.org/jcp/copyright.jsp

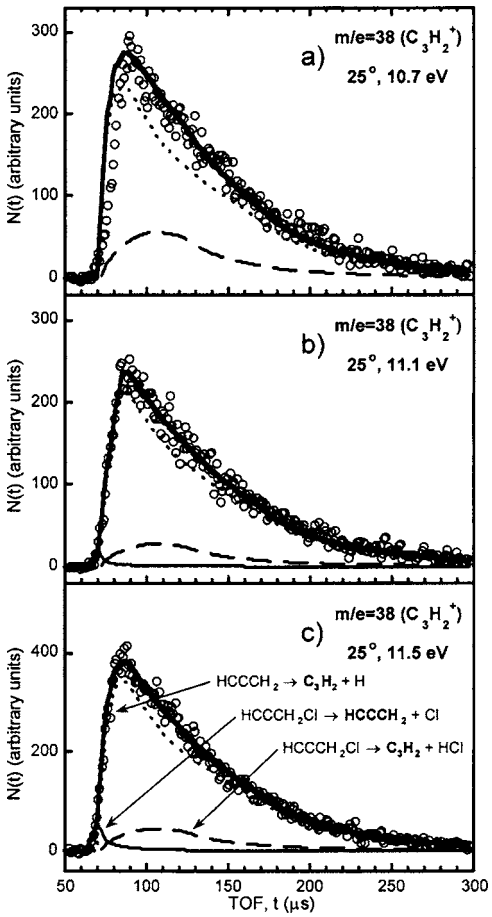

FIG. 8. TOF spectra of $m/e=38$ ($C_3H_2^+$) obtained at a 25° source angle for 200 000 laser shots with (a) 10.7 eV photoionization, (b) 11.1 eV photoionization, and (c) 11.5 eV photoionization. In each spectrum, open circles are experimental data and the bold solid line is the overall fit. The dotted line shows C_3H_2 produced by H loss from unstable C_3H_3 radicals. The dashed line is the contribution of C_3H_2 cofragments produced in HCl elimination of propargyl chloride. The thin solid line shows signal from dissociative ionization of stable C_3H_3 radicals.

process. This contribution is fairly obvious at 10.3 eV, but becomes obscured at higher ionization energies, as C–H fission is a minor channel compared to C–Cl fission in propargyl chloride.

Both the C–Cl bond fission and the HCl elimination channels of propargyl chloride contribute to the $m/e=38$ ($C_3H_2^+$) TOF spectra in Fig. 8. Some of the unstable nascent propargyl radicals may dissociate via one of the available H-loss channels: reactions (3)–(5). Loss of a hydrogen from the propargyl radical will not impart significant recoil velocity to the C_3H_2 cofragment, so the TOF distribution of the C_3H_2 products can be predicted by using the $P(E_T)$ for their parent C_3H_3 radicals, represented by the dotted line in Fig. 2. HCl elimination from propargyl chloride directly produces C_3H_2 by reaction (7). The specific C_3H_2 isomers produced in the initial HCl elimination cannot be identified. Furthermore, at least a portion of the C_3H_2 cofragments may be able to isomerize, as $E_{\text{available}}=121.8$ kcal/mol following the elimination step. Although we cannot determine how much energy is partitioned into vibrations of the HCl products, there is likely enough energy remaining to overcome the C_3H_2 isomerization barriers.[27] Figure 8 shows fits of $m/e=38$ data

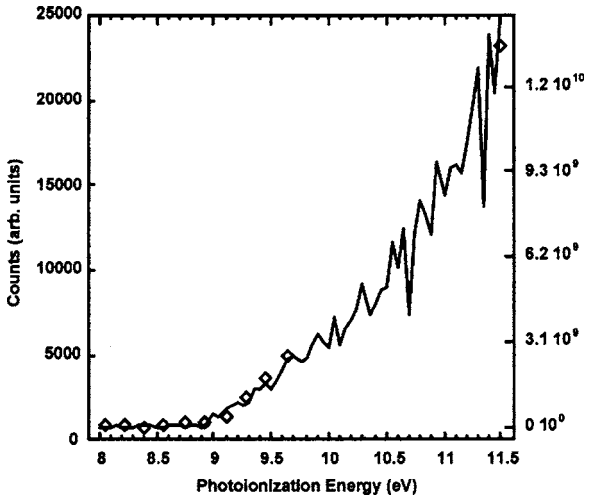

FIG. 9. Photoionization efficiency curve of $m/e=38$ data. The diamonds represent integrated $C_3H_2^+$ signal observed in this work. The solid line shows photoionization measurements in separate experiments by Taatjes *et al.* (Ref. 34) of C_3H_2 produced in a rich cyclopentene flame. Data are reproduced with permission.

obtained at three different ionization energies. In each spectrum, the dotted line shows C_3H_2 produced by C–H fission of propargyl radicals, fitted by the dotted line portion of the $P(E_T)$ in Fig. 2. The dashed line in Fig. 8 shows the distribution of C_3H_2 cofragments formed in HCl elimination, fitted by the $P(E_T)$ in Fig. 4. Stable C_3H_3 radicals may undergo dissociative ionization and appear in the $m/e=38$ TOF spectra as well, shown by the thin solid line in Figs. 8(b) and 8(c).

Choice of photoionization energy is critical in interpreting the $m/e=38$ TOF spectra. At 10.7 eV [Fig. 8(a)], the TOF distribution is not well fitted, but resembles that of $C_3H_3 \rightarrow C_3H_2+H$. The data in Fig. 8(a) are overfitted on the leading edge of the TOF peak, but this is not surprising. The fastest C_3H_2 products are the lowest in internal energy, so they may not be ionized as efficiently as C_3H_2 with higher internal energy, especially if the photoionization energy is close to the threshold. H_2CCC has an ionization potential of 10.43 eV, the highest of the three C_3H_2 isomers considered here.[40,45] Figure 8(b) shows a better fit of data taken at 11.1 eV. The quality of the fit is similar for data taken at 11.5 eV [Fig. 8(c)]. The progression of the shape of the TOF distribution with increasing photoionization energy suggests that H_2CCC is preferentially contributing on the fast side of the TOF distribution.

We integrated the signal at $m/e=38$ from 60 to 300 μs to obtain a low-resolution photoionization efficiency (PIE) curve for the C_3H_2 signal. This is shown in the open diamonds in Fig. 9. Surprisingly, the overall shape is very similar to that of the photoionization curve of C_3H_2 sampled from a rich cyclopentene flame by Taatjes *et al.*[34] shown in the solid line of Fig. 9. Although those authors used a Franck-Condon analysis to determine relative contributions of HCCCH and c-C_3H_2 in their data, we judge that it is unlikely that the unimolecular dissociation of propargyl would produce the same fraction of C_3H_2 products. To ascertain whether our observed photoionization efficiency curve is

Downloaded 25 Oct 2006 to 128.135.186.84. Redistribution subject to AIP license or copyright, see http://jcp.aip.org/jcp/copyright.jsp

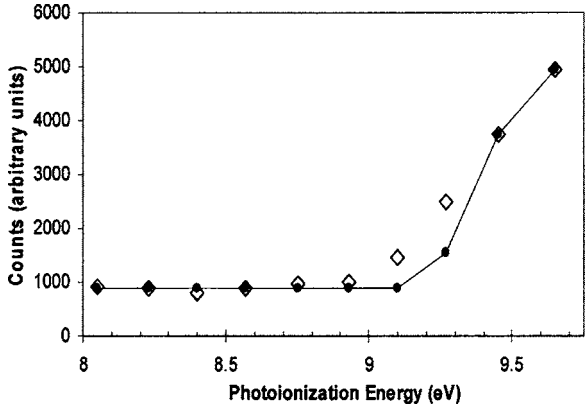

FIG. 10. Predicted photoionization efficiency curve of c-C_3H_2 for ionization energies used in this experiment. Points were predicted from Franck-Condon factors in Ref. 46. The solid dark circles connected by the solid line show predicted signal. The open diamonds show integrated $m/e=38$ signal observed in this work, also shown in Fig. 9.

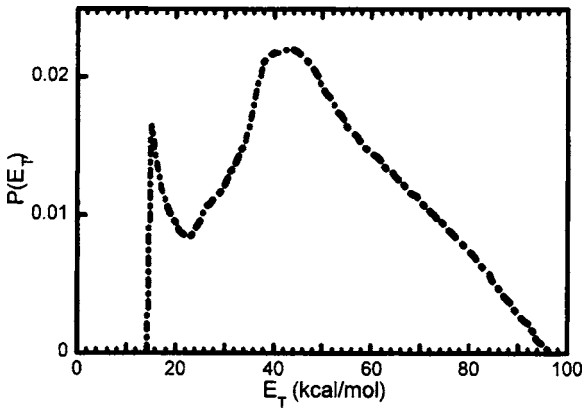

FIG. 12. Recoil translational energy distribution, $P(E_T)$, in initial C–H fission of propargyl chloride derived from forward convolution fitting of the data in Fig. 11. This distribution is only valid for C–H fission with $E_T \geqslant 15$ kcal/mol, as slower C_3H_2Cl products could not be detected.

consistent with the C_3H_2 products being in primarily the c-C_3H_2 isomer form, we used the Franck-Condon factors which fit the measured photoelectron spectrum of c-C_3H_2 reported by Clauberg *et al.*[40] to generate a prediction for the PIE curve taken at our resolution. This fit, shown in solid line with filled circles in Fig. 10, was generated using the Franck-Condon factors found by Clauberg[46] for c-C_3H_2. The photon energies were convoluted by the spread of energies inherent to the synchrotron at intervals of ~0.06 eV. The resulting predicted PIE curve for c-C_3H_2 is shown scaled and shifted vertically (to adjust for the small contamination from higher harmonics in our data taken at the NSRRC synchrotron) for comparison to our own PIE data. Our data points are shown by the open diamonds in the graph. The shape of the predicted PIE curve for c-C_3H_2 is similar to that of our data up to 9.7 eV, though our data appear to show an earlier onset. Interestingly, if one generates the c-C_3H_2 predicted PIE curve using the experimental photoionization spectrum of Clauberg *et al.*[40(b)] rather than the Franck-Condon factors they used to fit their spectrum, the comparison is even closer. (Chen discounted two small features at high photoelectron energies as not being from c-C_3H_2 isomers as he was not able to fit them in his Franck-Condon analysis.) No experimental photoionization spectrum of the HCCCH isomer has been measured, but the PIE curve predicted by Taatjes *et al.* for the HCCCH isomer is much flatter between 9.4 and 9.8 eV than our data. Thus we conclude that c-C_3H_2 is likely the dominant isomer formed in the unimolecular dissociation of propargyl radicals with energies near the unimolecular dissociation threshold. This is consistent with *ab initio* predictions of this isomer being the lowest in energy.

A minor C–H bond fission channel [reaction (8) or (9)] was observed in the initial photolysis of propargyl chloride. Figure 11 shows a forward convolution fit to the $m/e=73$ ($C_3H_2Cl^+$) data. Figure 12 shows the recoil kinetic energy distribution in C–H bond fission used to fit the data in Fig. 11. The E_T distribution is cut off at 14 kcal/mol, but this is not an accurate description of the C–H fission process. The data in Fig. 11 were taken at a source angle of 15°, prohibiting detection of C_3H_2Cl products from C–H fission with $E_T \leqslant 15$ kcal/mol. We attempted to measure the TOF spectrum at smaller source angles, but the signal was obscured by the background.

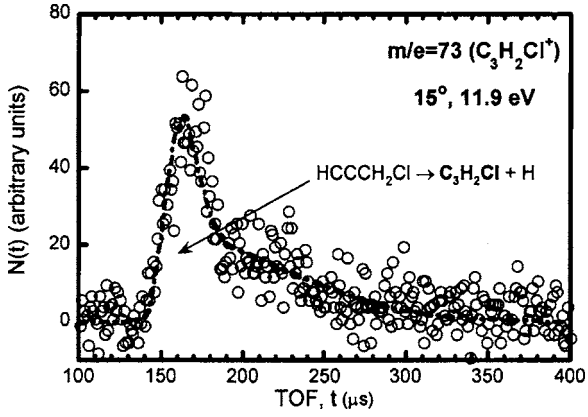

FIG. 11. TOF spectrum of $m/e=73$ ($C_3H_2Cl^+$) taken at a 15° source angle and 11.9 eV ionization energy for 300 000 laser shots. Open circles are experimental data points and the dot-dashed line is the forward convolution fit to the data.

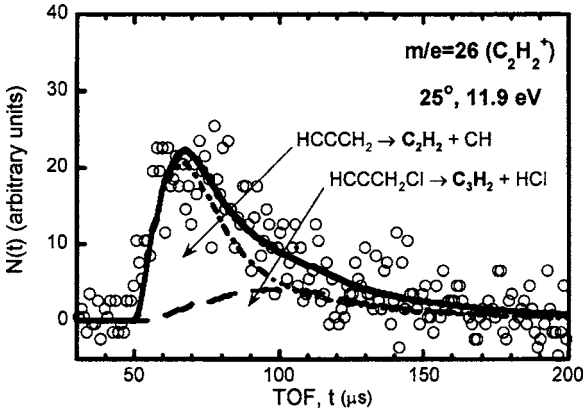

FIG. 13. TOF spectrum of $m/e=26$ ($C_2H_2^+$) taken at a 25° source angle and 11.9 eV ionization energy for 300 000 laser shots. Open circles are experimental data points and the bold solid line is the total fit to the data. The dot-dashed line shows signal attributed to dissociation of C_3H_3 radicals via reaction (6) due to multiphoton absorption of propargyl chloride. The dashed line shows dissociative ionization of C_3H_2 products from HCl elimination.

Downloaded 25 Oct 2006 to 128.135.186.84. Redistribution subject to AIP license or copyright, see http://jcp.aip.org/jcp/copyright.jsp

Signal in a $m/e=26$ ($C_2H_2^+$) TOF spectrum, Fig. 13, was assigned to C–C bond fission of propargyl radicals [reaction (6)]. Although the relative signal levels at 2.3 and 1.1 mJ laser pulse energies did not obviously indicate a multiphoton process, production of C_2H_2 is almost certainly due to multiphoton absorption by propargyl chloride, as the $m/e=26$ data could not be fitted in a manner consistent with the available energy. Indeed, the secondary $P(E_T)$ required to fit Fig. 13 has kinetic energy releases in excess of 25 kcal/mol. The dashed line in Fig. 13 shows where C_3H_2 cofragments in HCl elimination would appear if they underwent dissociative ionization to $C_2H_2^+$.

DISCUSSION

Photolysis of propargyl chloride at 157 nm resulted in C–Cl bond fission, HCl elimination, and a minor C–H fission channel. C–Cl bond fission produced propargyl radicals, some of which had sufficient internal energy to overcome the barriers to dissociation of the radical via C–H bond fission and H_2 elimination.

The data presented here allow for a determination of the lowest barrier to propargyl radical dissociation as the Cl atom TOF (Fig. 1) determines the internal energy of all nascent propargyl radicals and the C_3H_3 TOF (Fig. 5) indicates which of the radicals survive secondary dissociation. The internal energy range of the entire distribution of nascent propargyl radicals E_{int} is easily deduced from the momentum-matched Cl atom velocities using conservation of energy:

$$E_{parent} + h\nu = D_0(C-Cl) + E_{int} + E_{Cl} + E_T. \quad (10)$$

This calculation was done for the entire distribution of E_T in C–Cl bond fission for our experiment, shown in Fig. 2. The energy of a 157.6 nm photon $h\nu$ is equal to 181.3 kcal/mol. Our own RCCSD(T)/6-311+G(3*df*,2*p*) calculations[36,37] determined a bond energy of $D_0(C-Cl)=66.9$ kcal/mol. We chose the CCSD(T) method because it is the same method that was used by Nguyen *et al.*[25] to calculate the energetics for reactions (2)–(5). Therefore, any error in the calculated energy of the propargyl radical, used in our calculation of D_0, would also be present in energetics calculated for reactions (2)–(5); and the two errors would ultimately cancel. Thus, we do not use the higher C–Cl bond energy of 72 kcal/mol obtained in the complete basis set limit, as the calculation of the propargyl radical energy in Ref. 25, depicted in Fig. 14, is not in the complete basis set limit either. The comparison of experimental results with theoretical predictions is sensitive to the relative energies calculated for the propargyl chloride molecule, the C_3H_2 and C_3H asymptotic products, and the barriers to dissociation of the propargyl radical. E_{parent} is the internal energy of the propargyl chloride molecule; we estimated it by assuming that vibrational modes are not cooled by the nozzle expansion and have equilibrated to the nozzle temperature. Using vibrational modes calculated at the B3LYP/6-311+G** level of theory with the wave-number-linear scaling method,[47] the average vibrational energy of the propargyl chloride molecule was determined to be 2.1 kcal/mol at the 120 °C nozzle temperature used in our experiments. E_{Cl} refers to the energy of the spin-orbit state of the chlorine atoms. E_{Cl} is 0 kcal/mol if Cl is produced in the $^2P_{3/2}$ state and is 2.5 kcal/mol in the $^2P_{1/2}$ state.[48] The experiments presented here cannot distinguish between the two spin-orbit states, but 193 nm photolysis of propargyl chloride with resonance enhanced multiphoton ionization (REMPI) detection in separate experiments revealed that both $Cl(^2P_{3/2})$ and $Cl(^2P_{1/2})$ are produced.[35] E_T is the energy partitioned into translation of the propargyl radical and chlorine atom during initial C–Cl bond fission, measured in our experiments. The $m/e=39$ TOF spectra (Fig. 5) demonstrated which propargyl radicals do not undergo unimolecular dissociation. The corresponding $P(E_T)$ in Fig. 2 shows that $E_T=45$ kcal/mol marks the onset of dissociation of the unstable propargyl radicals. This corresponds to $E_{int}=71.5$ kcal/mol, our experimentally determined lowest barrier to dissociation.

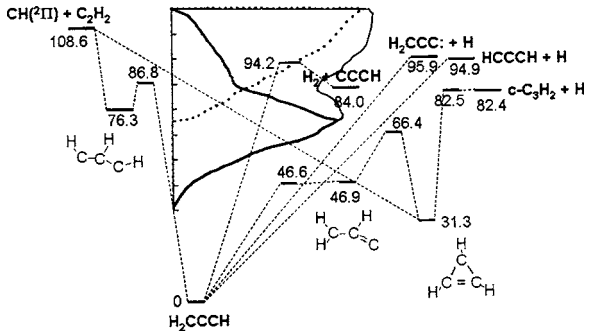

FIG. 14. The lowest-energy reaction paths for the three $H+C_3H_2$ and the H_2+HCCC product channels on the C_3H_3 potential energy surface calculated in Ref. 25 are shown overlaid with the internal energy distribution, determined from Eq. (10), for the nascent propargyl radicals in this experiment. All numbers indicate energies in kcal/mol. The first point of deviation of the thick solid line from the thin solid line depicts the experimentally determined lowest barrier height for the dissociation of the propargyl radical. It was assumed for the placement of the $P(E_{int})$ that the chlorine is formed in the spin-orbit ground state during initial C–Cl bond fission.

Figure 14 shows the experimentally measured internal energy distribution for nascent propargyl radicals superimposed on a portion of the $CH+C_2H_2$ potential energy surface calculated by Nguyen *et al.*[25] It is clear that the dissociation onset determined by our data for propargyl radicals is significantly lower than the energies of both the H_2+HCCC and the $H+C_3H_2$ product channels predicted at the CCSD(T) level of theory. In addition, the H_2+HCCC product channel has a significant exit barrier, unlike the other channels. In light of this, it is especially surprising that the HCCC products appear at the same energetic onset as the C_3H_2 products, that is, the internal energy distribution for unstable propargyl radicals shown in Fig. 2 fits both the $m/e=37$ and $m/e=38$ data.

The error associated with the experimentally determined barrier depends upon the error in fitting of the $m/e=39$ ($C_3H_3^+$) data. Figure 6 shows a worse, yet acceptable, fit to the data obtained by truncating the $P(E_T)$ at $E_T=40$ kcal/mol. Truncating the $P(E_T)$ at even lower energies gave unacceptable fits. The fit was less sensitive when the onset of dissociation was extended to values of E_T higher than 45 kcal/mol, as mentioned earlier in the Results and

Downloaded 25 Oct 2006 to 128.135.186.84. Redistribution subject to AIP license or copyright, see http://jcp.aip.org/jcp/copyright.jsp

Analysis. A nearly identical fit to that of Fig. 5 could be made by constructing a $P(E_T)$ where unimolecular dissociation onsets at E_T=50 kcal/mol. The fit was acceptable even with an onset at E_T up to 55 kcal/mol. Therefore, we assign error bars of +5/−10 kcal/mol to our E_{int} barrier determination. Our barrier value of E_{int}=71.5 kcal/mol is significantly lower than previously calculated dissociation barriers. Nguyen *et al.*[25] predicted that the lowest barrier to dissociation of propargyl radical (the c-C_3H_2+H product channel) is 82.5 kcal/mol, with an expected accuracy of 1–2 kcal/mol.

A substantial fraction of the propargyl radicals with internal energy above the dissociation barrier of 71.5 kcal/mol did not undergo dissociation. This is evidenced by the bold solid line in Fig. 2, which shows that the $P(E_T)$ for stable propargyl radicals extends to nearly E_T=0 kcal/mol. A possible explanation for the stability of the high internal energy radicals (formed with low E_T) is that they are formed in an excited state. Excited-state radicals may fluoresce, precluding dissociation, or the process of internal conversion may be so slow that the propargyl radicals are detected before they can dissociate. The bimodal nature of the total $P(E_T)$ in Fig. 2 also suggests that the C–Cl bond fission events of low kinetic energy produced propargyl radicals in an excited state. Nguyen *et al.*[25] predicted the first excited state of propargyl at 57.1 kcal/mol above the ground state, accessible to many of the nascent radicals produced in these experiments. MRCI calculations by Eisfeld found vertical excitation energies and potential energy surfaces for several excited states.[49] The results predict that the propargyl's absorption spectrum is dominated by the $2\,^2B_1 \leftarrow 1\,^2B_1$ transition, but do not confirm strong absorption at 242 nm.

It is possible that a significant fraction of the available energy is partitioned into rotation of the propargyl radical during C–Cl bond fission of propargyl chloride. A simple calculation using the rigid-radical impulsive dissociation model showed that high rotational energies are expected. For C–Cl bond fission events with E_T=43 kcal/mol, at the peak of the $P(E_T)$ in Fig. 2, the propargyl radical is predicted to have 22 kcal/mol imparted to rotation. Such high rotational energies should add a centrifugal barrier to the dissociation of propargyl, but our experimentally determined barrier is lower than expected, not higher. The rigid-radical impulsive model may not be appropriate for propargyl chloride because it assumes that the molecule is dissociating from its ground-state geometry. There is not enough evidence to support or refute the validity of this assumption for the 157 nm photolysis of propargyl chloride.

The experimentally determined barrier of 71.5 (+5/−10) kcal/mol is even lower than the predicted overall reaction enthalpies for the dissociation channels of the propargyl radical. The c-C_3H_2+H products are predicted to be the most stable at 82.4 kcal/mol relative to the propargyl radical.[25] Thus our results disagree with both the theoretically predicted dissociation barrier heights and the product energies. Good agreement relies on not only an accurate theoretical treatment of the energetics of the CCCH and C_3H_2 product channels with respect to propargyl radical but also a good C–Cl bond energy in the photolytic precursor, which has not been experimentally determined. Note that the energetics of the c-C_3H_2+H channel can also be estimated from the experimental ΔH_f^0 for c-C_3H_2 (making the small correction to 0 K) and propargyl radicals;[39,45,50] this gives a bond dissociation energy of 89.5 kcal/mol for the c-C_3H_2 product channel, considerably higher than both the theoretical results referenced here and the lower onset detected in our experiments. Although theoretical methods such as CCSD(T) may become less reliable for biradical and triradical species such as HCCCH and CCCH, the c-C_3H_2 has a large singlet-triplet splitting,[30,40] so it is reasonable to expect the calculations to be accurate. Furthermore, preliminary MRCI calculations in Mebel's group give energies close to the CCSD(T) calculations.[51] Similar results on the H_2+CCCH product channel have been obtained by Varner and Stanton.[52] Nevertheless, using the calculated C–Cl bond energy, the low onset for dissociation of propargyl radicals was apparent in both our photoionization data and in our electron bombardment data. As numerous prior experiments in our group using the same methodology have given energies to within 2 kcal/mol of the theoretically predicted barriers in other systems, we felt it important to report our results to inform future investigators of the disagreement on this system in the hopes that it can be resolved.

ACKNOWLEDGMENTS

This work was supported by the Chemical, Geosciences and Biosciences Division, Office of Basic Energy Sciences, Office of Science, U.S. Department of Energy, under Grant No. DE-FG02-92ER14305 (L.J.B.). Synchrotron beamtime and additional funding were provided by the National Synchrotron Radiation Research Center and Academia Sinica in Taiwan (J.J.L.). Shih-Huang Lee and Chanchal Chaudhuri are acknowledged for technical assistance during the experiments. The authors thank Craig Taatjes for sharing photoionization efficiency data discussed in this paper, and also Alexander Mebel for providing calculated energies presented in Fig. 14. The authors most sincerely thank Y. T. Lee for his intelligent guidance.

[1] R. I. Kaiser, Y. T. Lee, and A. G. Suits, J. Chem. Phys. **105**, 8705 (1996).
[2] R. I. Kaiser and A. M. Mebel, Int. Rev. Phys. Chem. **21**, 307 (2002).
[3] H. Matthews and W. M. Irvine, Astrophys. J. Lett. **298**, L61 (1985).
[4] P. Thaddeus, J. M. Vrtilek, and C. A. Gottlieb, Astrophys. J. Lett. **299**, L63 (1985).
[5] J. Cernicharo, C. Kahane, M. Guelin, and J. Gomez-Gonzalez, Astron. Astrophys. **189**, L1 (1988).
[6] S. Yamamoto, S. Saito, M. Ohishi, H. Suzuki, S. Ishikawa, N. Kaifu, and A. Murakami, Astrophys. J. Lett. **322**, L55 (1987).
[7] R. I. Kaiser, C. Ochsenfeld, D. Stranges, M. Head-Gordon, and Y. T. Lee, Faraday Discuss. **109**, 183 (1998).
[8] J. A. Miller and C. F. Melius, Combust. Flame **91**, 21 (1992).
[9] D. A. Ramsay and P. Thistlethwaite, Can. J. Phys. **44**, 1381 (1966).
[10] M. S. Robinson, M. L. Polak, V. M. Bierbaum, C. H. DePuy, and W. C. Lineberger, J. Am. Chem. Soc. **117**, 6766 (1995).
[11] F. P. Lossing, Can. J. Chem. **50**, 3973 (1972).
[12] T. Gilbert, R. Pfab, I. Fischer, and P. Chen, J. Chem. Phys. **112**, 2575 (2000).
[13] K.-C. Lau and C. Y. Ng, J. Chem. Phys. **122**, 224310 (2005).
[14] T. Zhang, X. N. Tang, K.-C. Lau *et al.*, J. Chem. Phys. **124**, 074302 (2006).
[15] J. C. Robinson, N. E. Sveum, and D. M. Neumark, J. Chem. Phys. **119**, 5311 (2003).
[16] E. B. Jochnowitz, X. Zhang, M. R. Nimlos, M. E. Varner, J. F. Stanton, and G. B. Ellison, J. Phys. Chem. A **109**, 3812 (2005).

Downloaded 25 Oct 2006 to 128.135.186.84. Redistribution subject to AIP license or copyright, see http://jcp.aip.org/jcp/copyright.jsp

[17] A. Fahr, P. Hassanzadeh, B. Laszlo, and R. E. Huie, Chem. Phys. **215**, 59 (1997).
[18] M. Zierhut, B. Noller, T. Schultz, and I. Fischer, J. Chem. Phys. **122**, 094302 (2005).
[19] M. Wyss, E. Riaplov, and J. P. Maier, J. Chem. Phys. **114**, 10355 (2001).
[20] H.-J. Deyerl, I. Fischer, and P. Chen, J. Chem. Phys. **111**, 3441 (1999).
[21] T. L. Nguyen, A. M. Mebel, S. H. Lin, and R. I. Kaiser, J. Phys. Chem. A **105**, 11549 (2001).
[22] L. Vereecken, K. Pierloot, and J. Peeters, J. Chem. Phys. **108**, 1068 (1998).
[23] L. Vereecken and J. Peeters, J. Phys. Chem. A **103**, 5523 (1999).
[24] R. Guadagnini, G. C. Schatz, and S. P. Walch, J. Phys. Chem. A **102**, 5857 (1998).
[25] T. L. Nguyen, A. M. Mebel, and R. I. Kaiser, J. Phys. Chem. A **105**, 3284 (2001).
[26] W. M. Jackson, D. S. Anex, R. E. Continetti, B. A. Balko, and Y. T. Lee, J. Chem. Phys. **95**, 7327 (1991).
[27] A. M. Mebel, W. M. Jackson, A. H. H. Chang, and S. H. Lin, J. Am. Chem. Soc. **120**, 5751 (1998).
[28] R. H. Qadiri, E. J. Feltham, E. E. H. Cottrill, N. Taniguchi, and M. N. R. Ashfold, J. Chem. Phys. **116**, 906 (2002).
[29] R. H. Qadiri, E. J. Feltham, N. H. Nahler, R. P. Garcia, and M. N. R. Ashfold, J. Chem. Phys. **119**, 12842 (2003).
[30] M. Rubio, J. Stalring, A. Bernhardsson, R. Lindh, and B. O. Roos, Theor. Chem. Acc. **105**, 15 (2000).
[31] R. A. Seburg, E. V. Patterson, J. F. Stanton, and R. J. McMahon, J. Am. Chem. Soc. **119**, 5847 (1997).
[32] C. Ochsenfeld, R. I. Kaiser, Y. T. Lee, A. G. Suits, and M. Head-Gordon, J. Chem. Phys. **106**, 4141 (1997).
[33] V. Jonas, M. Bohme, and G. Frenking, J. Phys. Chem. **96**, 1640 (1992).
[34] C. A. Taatjes, S. J. Klippenstein, N. Hansen, J. A. Miller, T. A. Cool, J. Wang, M. E. Law, and P. R. Westmoreland, Phys. Chem. Chem. Phys. **7**, 806 (2005).
[35] L. R. McCunn, D. I. G. Bennett, L. J. Butler, H. Fan, F. Aguirre, and S. T. Pratt, J. Phys. Chem. A **110**, 843 (2006).
[36] We calculated the C–Cl bond energy by the CCSD(T) method using MOLPRO. The method is the same used by Nguyen *et al.* in Ref. 25. Therefore, any error in our calculated energy of the propargyl radical would also be present in their calculation and thus would cancel out.
[37] H.-J. Werner, P. J. Knowles, M. Schütz *et al.*, MOLPRO, a package of *ab initio* programs.
[38] To calculate the energy required for HCl elimination, we added the energies for reactions (1) and (3) to get $\Delta H_{0\ \mathrm{K}}$ for $HCCCH_2Cl \rightarrow HCCCH+H+Cl$, which were both calculated by CCSD(T) methods. We then added $\Delta H_{0\ \mathrm{K}}$ for $H+Cl \rightarrow HCl$ from H. M. Rosenstock, K. Draxl, B. W. Steiner, and J. T. Herron, J. Phys. Chem. Ref. Data Suppl.6, 1 (1977). The result for HCl elimination is $\Delta H_{0\ \mathrm{K}} = 66.9 + 94.9 + -102.3 = 59.5$ kcal/mol.
[39] J. W. Hudgens and C. Gonzalez, J. Phys. Chem. A **106**, 6143 (2002).
[40] (a) H. Clauberg, D. W. Minsek, and P. Chen, J. Am. Chem. Soc. **114**, 99 (1992); (b) H. Clauberg and P. Chen, J. Phys. Chem. **96**, 5676 (1992).
[41] J. W. Gallagher, C. E. Brion, J. A. R. Samson, and P. W. Langhoff, J. Phys. Chem. Ref. Data **17**, 9 (1988).
[42] B. Ruscic and J. Berkowitz, Phys. Rev. Lett. **50**, 675 (1983). Ruscic's relative photoionization cross section gives 28 Mb at 14.8 eV when renormalized in accordance with the 34.2 Mb value beyond the 1 S threshold given by Berkowitz [*Atomic and Molecular Photoabsorption: Absolute and Total Cross Sections* (Academic, San Diego, 2002)]. A recent measurement by R. Flesch J. Plenge, S. Kühl, M. Klusmann, and E. Rühl [J. Chem. Phys. **117**, 9663 (2002)] lies close to this.
[43] J. C. Robinson, N. E. Sveum, S. J. Goncher, and D. M. Neumark, Mol. Phys. **103**, 1765 (2005).
[44] S. Ikuta, J. Chem. Phys. **106**, 4536 (1997).
[45] K.-C. Lau and C. Y. Ng, Chin. J. Chem. Phys. **19**, 29 (2006).
[46] H. Clauberg, Ph.D. thesis, Harvard University, 1992.
[47] H. Yoshida, K. Takeda, J. Okamura, A. Ehara, and H. Matsuura, J. Phys. Chem. A **106**, 3580 (2002).
[48] P. B. Davies and D. K. Russell, Chem. Phys. Lett. **67**, 440 (1979).
[49] W. Eisfeld, J. Phys. Chem. A **110**, 3903 (2006).
[50] L. J. Chyall and R. R. Squires, Int. J. Mass Spectrom. Ion Process. **149/150**, 257 (1995).
[51] A. Mebel (private communication).
[52] M. Varner and J. F. Stanton (private communication).

Downloaded 25 Oct 2006 to 128.135.186.84. Redistribution subject to AIP license or copyright, see http://jcp.aip.org/jcp/copyright.jsp